Nonpolar Environment of Tryptophans in Erythrocyte Water Channel CHIP28 Determined by Fluorescence Quenching†

Javier Farinas,‡ Alfred N. Van Hoek, Lan-Bo Shi, Christopher Erickson, and A. S. Verkman*

Departments of Medicine and Physiology, Cardiovascular Research Institute, and Graduate Group in Biophysics, University of California, San Francisco, California 94143-0532

Received March 5, 1993; Revised Manuscript Received August 26, 1993®

ABSTRACT: CHIP28 is an abundant water-transporting protein in erythrocytes, kidney proximal tubule, and other fluid-transporting tissues. To determine the environment of the four tryptophans in CHIP28, fluorescence spectra and quenching by polar and nonpolar compounds were measured in stripped human erythrocyte membranes containing CHIP28 and in proteoliposomes reconstituted with purified CHIP28; comparative studies were performed in membranes containing MIP26. Functional analysis showed that CHIP28 water permeability was not affected by the polar quenchers iodide and acrylamide nor the nonpolar *n*-anthroyloxy fatty acids (*n*-AF). The emission maximum of CHIP28 tryptophan fluorescence was at 324 ± 2 nm and did not change with the addition of quenchers; the maximum for MIP26 was at 335 ± 5 nm. There was weak quenching of CHIP28 tryptophan fluorescence by the polar compounds iodide and acrylamide, with Stern–Volmer constants of 0.13 and 0.71 M^{-1}, respectively. $HgCl_2$ inhibited water permeability by >95% at 50 μM and quenched CHIP28 fluorescence reversibly by up to 70% with a biphasic concentration dependence; quenching by $HgCl_2$ and acrylamide was not additive. The membrane-associated *n*-AF probes quenched CHIP28 fluorescence by up to 80% with the greatest quenching for $n = 2$ and 12; addition of $HgCl_2$ or acrylamide after *n*-AF caused a small, anthroyloxy-position-dependent increase in quenching which was greatest at $n = 6$. These studies indicate that the tryptophans in CHIP28 are in a nonpolar, membrane-associated environment. Mathematical modeling of the *n*-AF results suggests that the tryptophans are clustered near the surface and center of the bilayer. Site-directed mutagenesis of the highly conserved tryptophan 210 to leucine had no significant effect on the CHIP28 water-transport function, as assayed in *Xenopus* oocytes. These results provide new information about CHIP28 and MIP26 structure that was not anticipated from the analysis of hydropathy.

CHIP28 is the major water-transporting protein in erythrocytes, kidney proximal tubule, thin descending limb of Henle, and a number of fluid-transporting cells in lung, intestine, eye, and other tissues (Preston & Agre, 1991; Preston et al., 1992; Sabolic et al., 1992; Zhang et al., 1993a; Hasegawa et al., 1993). CHIP28 functions as a selective water transporter that excludes urea, protons, and monovalent ions (Preston et al., 1992; Van Hoek & Verkman, 1992; Zeidel et al., 1992; Zhang et al., 1993a). On the basis of biophysical studies showing that CHIP28 has high water permeability, a ratio of osmotic-to-diffusional water permeability of >1, and a low Arrhenius activation energy, it is likely that CHIP28 contains a continuously open aqueous pathway with a diameter of ~2 Å. CHIP28 is probably assembled in the membrane as tetramers (Smith & Agre, 1991; Verbavatz et al., 1993) containing functional monomeric subunits (Van Hoek et al., 1991; Preston et al., 1993; Zhang et al., 1993b).

As described in the preceding article, hydropathy analysis indicates that CHIP28 is a very hydrophobic protein, with up to eight possible membrane-spanning domains (Van Hoek et al., 1993). Figure 1 gives a hydropathy plot and schematic diagram of CHIP28 topology showing the first and last membrane-spanning domains; the internal spanning domains and extramembrane connecting segments are not shown because their topology has not been established. The N- and C-termini are oriented cytoplasmically, and the asparagine

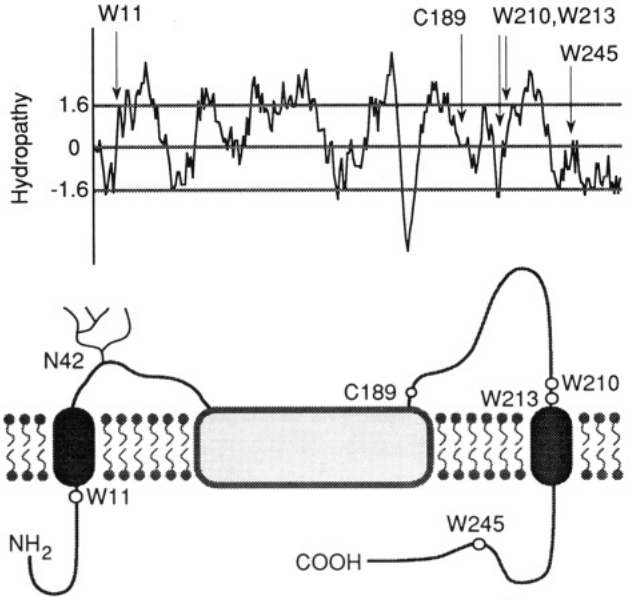

FIGURE 1: Locations of tryptophans in the CHIP28 water channel. The four tryptophans (W) in CHIP28 are indicated in the hydropathy (top) and membrane topology (bottom) plots. The glycosylation site (N42) and cysteine 189 (C189) are also indicated. Of the eight possible membrane-spanning domains, only the first and last are shown because the locations of the other domains have not been established and need not be specified to depict the locations of the four tryptophans. See the text for details.

† This work was supported by Grants DK35124 and DK43840 from the National Institutes of Health and a grant-in-aid from the American Heart Association. A.S.V. is an established investigator of the American Heart Association.

* Address correspondence to this author at the Cardiovascular Research Institute.

‡ Graduate Group in Biophysics.

® Abstract published in *Advance ACS Abstracts,* October 15, 1993.

0006-2960/93/0432-11857$04.00/0

residue 42 (N42) is glycosylated in a fraction of CHIP28 monomers (Preston & Agre, 1991; Zhang et al., 1993a). Site-directed mutagenesis of the four cysteine residues indicates that cysteine 189 (C189) is the site of action of mercurial inhibitors and probably resides at or near the aqueous pore (Preston et al., 1993; Zhang et al., 1993b). There are four tryptophan residues in CHIP28 (W11, W210, W213, and W245). W11, W210, and W213 are predicted to lie just on the edges of hydrophobic segments, and W245 is predicted to lie in the cytoplasmic C-terminus. Note that the predicted locations for the four tryptophans do not depend on the details of the internal domains. The homologous protein MIP26 contains five tryptophans; sequence alignment of a series of MIP family proteins (MIP26, CHIP28, NOD26, TIP, TUR, Tob, BiB, and GLP; Wistow et al., 1991) indicates that W210 and W213 are highly conserved (W210 and W213 of CHIP28 correspond to W202 and W205 of MIP26), that W11 is slightly conserved (W11 of CHIP28 corresponds to W10 of MIP26 and to W65 of BiB), and that W245 of CHIP28 is not conserved.

The purpose of this study was to probe the environment of tryptophan residues in CHIP28 for comparison with structural predictions of hydropathy analysis. The tryptophan environment was examined by spectral analysis of purified CHIP28 in membranes and by fluorescence quenching using the polar compounds iodide and acrylamide (Eftink & Ghiron, 1976) and the lipophilic membrane-associated *n*-anthroyloxy fatty acids (*n*-AF),[1] in which the anthroyloxy chromophore is positioned at specified depths in the bilayer (Kleinfeld & Lukacovic, 1985). Contrary to the predictions of hydropathy analysis, it was found that the tryptophans in CHIP28 were in a nonpolar environment within the bilayer. Interestingly, the water-transport inhibitor $HgCl_2$ was a potent quencher of tryptophan fluorescence. The fluorescence data, taken together with CHIP28 sequence and structural information, were used to establish constraints on models for CHIP28 structure. In addition, site-directed mutagenesis was used to determine whether the highly conserved tryptophan 210 in CHIP28 is critical for its water-transporting function.

MATERIALS AND METHODS

Materials. CHIP28-containing vesicles were prepared from human erythrocytes as described by Van Hoek and Verkman (1992). *N*-Lauroylsarcosine-stripped membrane vesicles were prepared either directly from erythrocyte ghosts or from ghosts treated with EDTA and KI to yield inside-out vesicles. Stock solutions of vesicles (1 mg of protein/mL, lipid-to-protein ratio 15 g/g) were stored at 4 °C. Reconstituted proteoliposomes containing either CHIP28 or MIP26 were prepared as described in the preceding article (Van Hoek et al., 1993). Stock solutions of 3 M acrylamide, 4 M KI (containing 1 mM sodium thiosulfate to prevent the oxidation of iodide), and 1.25 mM $HgCl_2$ were prepared in water. The *n*-anthroyloxy fatty acid (*n*-AF) probes [2-, 3-, 6-, 9-, and 12-(9-anthroyloxy)-stearic acid and 16-(9-anthroyloxy)palmitic acid] were obtained from Molecular Probes, Inc. (Eugene, OR), and stored as 10 mM stock solutions in ethanol at −20 °C.

Functional Assays. The osmotic water permeability (P_f) of vesicles containing CHIP28 was measured by a stopped-flow light-scattering assay (Van Hoek & Verkman, 1992). The effects of quenchers on P_f were measured at 10 °C. The permeability of vesicles to the solutes KI and acrylamide was measured at 23 °C from the time course of scattered light intensity in response to 300 mM solute gradients.

Fluorescence Measurements. Steady-state fluorescence intensity was measured on an SLM 8000c fluorimeter (SLM Instruments, Urbana, IL). The fluorescence signal was normalized to a quantum counter in the reference channel. Excitation light at either 280 or 295 nm was obtained from a Hg–Xe arc lamp and a grating monochrometer with a 4-nm slit width. Emitted fluorescence was detected at 90° by a photomultiplier after it passed through a monochrometer with a 2-nm slit width (for spectral measurements) or an 8-nm slit width (for quenching experiments). The fluorescence signal was corrected for dilution, background, and inner-filter effect (Hill et al., 1986). Background signal (<1% of total signal) was subtracted using the signal of a blank containing no membranes. There was no significant contribution of scattering from membranes to the signal. Because of the narrow width of the Raman scattering peak (~20 nm), spectra were unaffected in the region of interest (>320 nm) with the use of 2 nm slits. The correction for the inner-filter effect was $F_c = F \text{ antilog } [(A_{ex} + A_{em})/2]$, where F_c and F are the corrected and uncorrected fluorescence intensities, respectively, and A_{ex} and A_{em} are the sample absorbances at the excitation and emission wavelengths, respectively. Absorption spectra were measured on a HP8452 photodiode array spectrophotometer (Hewlett-Packard). All fluorescence measurements were made at room temperature.

Quenching Experiments. CHIP28-containing vesicles or proteoliposomes were diluted to a concentration of 5 μg/mL with 10 mM sodium phosphate (pH 7.4) buffer containing 0.1 mM EDTA. No EDTA was used for the experiments with $HgCl_2$. Small aliquots of the stock solutions of quenchers were added to stirred vesicle suspensions. Fluorescence intensity was measured after the signal had stabilized: 30 s for KI or acrylamide, up to 30 min for $HgCl_2$, and overnight for the *n*-AF compounds. The samples were excited at 280 nm, except for the acrylamide experiments which were conducted at 295 nm; the emission wavelength was 350 nm. The ethanol vehicle added with the anthroyloxy probes (<2% of the total volume) did not affect CHIP28 fluorescence.

Data Analysis. The effect of quenchers on tryptophan fluorescence was analyzed with the Stern–Volmer equation: $F_o/F = 1 + K_q[Q]$, where F and F_o are the fluorescence intensities with and without quencher, [Q] is the quencher concentration, and K_q is the Stern–Volmer constant. K_q was determined by least-squares linear regression. For Stern–Volmer plots which displayed curvature, K_q was calculated as the slope at zero quencher concentration. For the anthroyloxy probe experiments, energy-transfer efficiencies (E) were calculated by the equation $E = 1 - F/F_o$.

Site-Directed Mutagenesis. cDNA encoding human CHIP28 was obtained by PCR amplification using human kidney cortex cDNA as template, sense primer 5′-GCCAC-CATGGCCAGCGAGTTCAAGAAGAAG-3′, and antisense primer 5′-GCCGGATCCCTTCTATTTGGGCTTCATCTC-3′. The PCR product was subcloned in SP64 (containing the 5′-untranslated *Xenopus* globin enhancer) at *Nco*I and *Bam*HI sites (Zhang et al., 1993a) and then subcloned in pSELECT1 at *Hind*3 and *Bam*HI sites. Mutagenesis was carried out as described by Zhang et al. (1993b) using the antisense mutagenic oligonucleotide, 5′-CA GAA AAT CAA GTG GTT GC-3′, corresponding to bases +620 to +638 of CHIP28,

[1] Abbreviations: *n*-AF, fatty acid labeled with anthroyloxy at the *n* position of the hydrocarbon chain; P_f, osmotic water permeability; F, fluorescence intensity; K_q, Stern–Volmer quenching constant; Q, quencher; E, fluorescence energy-transfer efficiency; $K_{1/2}$, affinity constant.

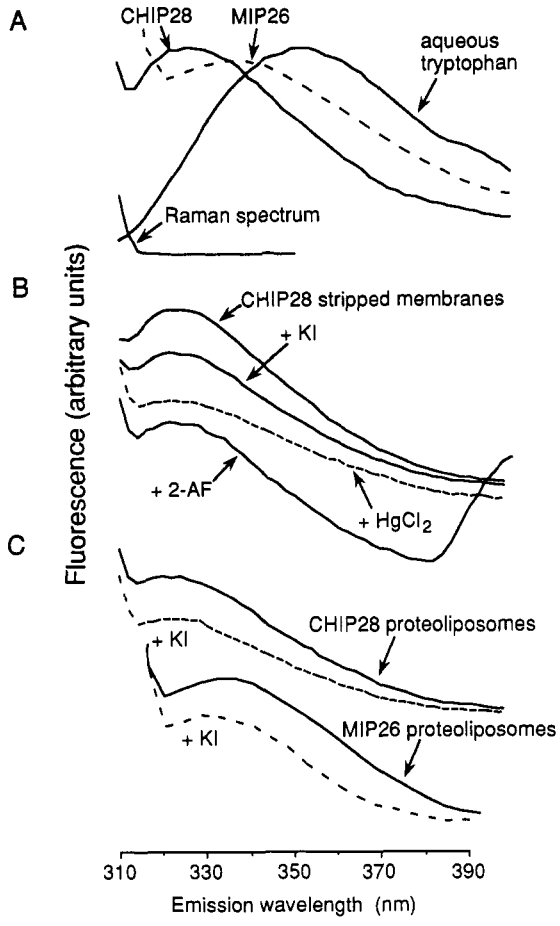

FIGURE 2: Tryptophan fluorescence spectra of CHIP28 and MIP26. The spectra were obtained as described in Materials and Methods. (A) Spectra of tryptophan (100 mM) and reconstituted CHIP28 (5 μg/mL) and MIP26 (1 μg/mL) in 10 mM sodium phosphate, pH 7.4. The Raman scattering peak is shown for comparison. (B) Spectra of CHIP28 in stripped membranes (5 μg/mL) in the presence of KI (0.67 M), $HgCl_2$ (1 mM), and 2-AF (3.3 μM). (C) Spectra of reconstituted CHIP28 (1 μg/mL) and MIP26 (1 μg/mL) in proteoliposomes with and without KI (0.67 M). Spectra in B and C were displaced in the y-direction for clarity (without a change in amplitude).

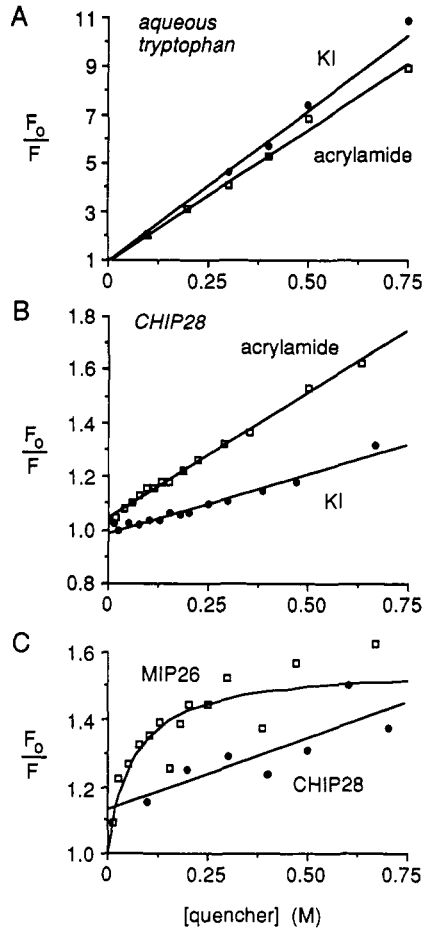

FIGURE 3: Quenching of tryptophan fluorescence by iodide and acrylamide. (A) Stern–Volmer plot for the quenching of tryptophan (100 μM) in water by KI and acrylamide. (B) Stern–Volmer plot for the quenching of CHIP28 (5 μg/mL) in stripped membranes by KI and acrylamide. (C) Stern–Volmer plot for the quenching of reconstituted CHIP28 (1 μg/mL) and MIP26 (1 μg/mL) by KI. F_o/F values were determined and corrected as described in Materials and Methods. Averaged Stern–Volmer constants are given in the text.

where the underlined A gave the tryptophan-to-leucine mutation (W210L). Wild-type and mutant cDNAs were confirmed by sequence analysis. For expression studies, defolliculated *Xenopus* oocytes were injected with 50 nL of water or *in vitro* transcribed/capped cRNA (0.1 mg/mL) encoding wild-type or mutant CHIP28, as described previously (Zhang et al., 1993a). Oocyte water permeability was assayed at 10 °C from the rate of swelling after a 20-fold dilution of the extracellular Barth's buffer with distilled water.

RESULTS

Figure 2A shows the fluorescence emission spectra of intrinsic tryptophans in CHIP28 and MIP26. The excitation wavelength was 280 nm to minimize the signal contribution from the Raman scattering peak. For more concentrated samples in which the Raman peak was very small, the emission spectrum was not affected by excitation wavelengths in the range 280–295 nm, indicating no significant contribution from tyrosine fluorescence. In proteins, tyrosine has a lower quantum yield, a lower extinction coefficient, and blue-shifted emission and excitation spectra compared to tryptophan (Lakowicz, 1983). Therefore, the lack of a contribution from tyrosine to the CHIP28 fluorescence spectrum is not surprising. The emission maximum for CHIP28 was at 324 ± 2 nm for CHIP28 in native, *N*-lauroylsarcosine-stripped membranes and reconstituted proteoliposomes. For comparison, the emission maximum was at 352 nm for an aqueous solution of tryptophan and at 335 ± 5 nm for MIP26 in reconstituted proteoliposomes. The position of the emission maximum for CHIP28 was not influenced by the addition of the iodide, *n*-AF compounds, or $HgCl_2$ quenchers (Figure 2B), whereas the emission maximum for MIP26 was blue-shifted to 327 nm after the addition of iodide (Figure 2C). These results suggest that the tryptophans in CHIP28 are located in a nonpolar environment (see the Discussion).

The aqueous-phase compounds iodide and acrylamide quench the fluorescence of protein tryptophans that are in an accessible polar environment. Figure 3 shows Stern–Volmer plots for the quenching of CHIP28, MIP26, and aqueous tryptophan fluorescence. Whereas aqueous tryptophan was quenched strongly by iodide and acrylamide with K_q = 12.4 and 10.9 M^{-1}, respectively (Figure 3A), there was no significant quenching of CHIP28 tryptophan fluorescence by iodide (K_q = 0.13 ± 0.3 M^{-1}, SEM, n = 7) and relatively little quenching by acrylamide (K_q = 0.71 ± 0.3 M^{-1}, n = 5) (Figure 3B). These results support the conclusion that the tryptophans of CHIP28 in *N*-lauroylsarcosine-stripped membranes and in reconstituted proteoliposomes (Figure 3C) are located in a nonpolar environment. There was relatively greater quenching

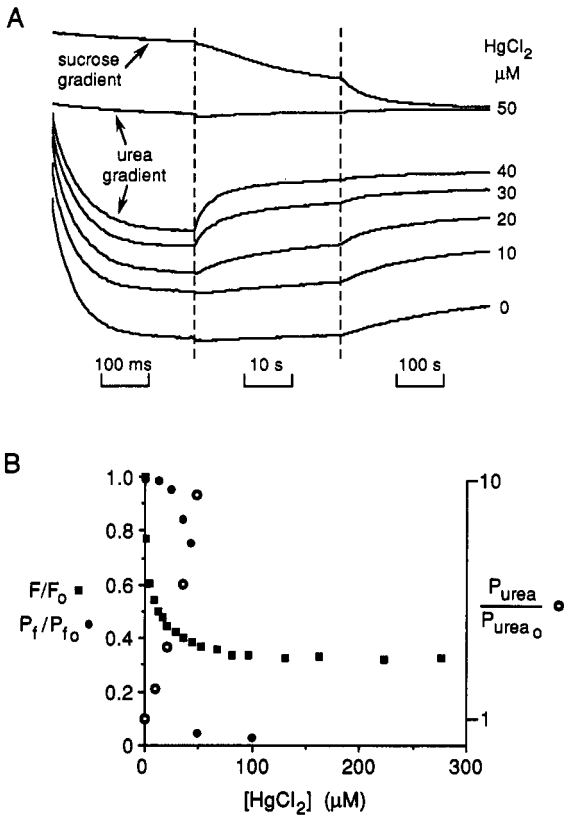

FIGURE 4: Effect of $HgCl_2$ on CHIP28 function and tryptophan fluorescence quenching. (A) Effect of $HgCl_2$ on osmotic water and urea permeability in CHIP28-containing stripped vesicles. Vesicles in a 220 mM NaCl buffer were subjected to a 300 mM inwardly directed gradient of sucrose or urea at 10 °C. Vesicles were incubated with the indicated concentrations of $HgCl_2$ for 30 min prior to measurements (see the text for details). (B) Relative tryptophan fluorescence (F/F_o, ■), osmotic water permeability ($P_f/P_{f,o}$, ●), and urea permeability ($P_{urea}/P_{urea,o}$, ○) as a function of $HgCl_2$ concentration.

of MIP26 tryptophan fluorescence by iodide with K_q = 2.2 M^{-1} (Figure 3C), suggesting that one or more tryptophans are in a polar environment.

Water permeability measurements were carried out to determine whether CHIP28 remains functional in the presence of iodide, acrylamide, and the anthroyloxy probes. In the presence of an NaCl gradient, the calculated osmotic water permeability (P_f, in cm/s) was 0.032 ± 0.005. The addition of a high concentration of 12-AF had no effect on P_f (0.034 ± 0.006). Replacement of NaCl by KI or acrylamide also had no significant effect (KI, 0.035 ± 0.003; acrylamide, 0.031 ± 0.008), indicating that the polar quenching compounds did not affect CHIP28 function and probably did not cause a gross change in CHIP28 conformation. When vesicles were subjected to a 300 mOsm inwardly directed gradient of KI or acrylamide, there was initial osmotic water efflux, followed by slower solute influx. Solute influx was >50% complete in <1 min under the conditions of the fluorescence experiments, indicating that these quenchers were present on both the internal and external membrane surfaces.

Mercurial compounds are the only known inhibitors of the CHIP28 water channel (Verkman, 1992). They are thought to bind covalently to sulfhydryl groups on cysteines to block the aqueous pore directly or to alter CHIP28 conformation. Because Hg^{2+} is known to quench the fluorescence of tryptophan (Chen, 1971), we examined the quenching of intrinsic CHIP28 tryptophan fluorescence by $HgCl_2$. Figure 4A shows the inhibition of P_f by $HgCl_2$ in the CHIP28 vesicles. The inhibition is observed by the decrease in initial curve slope at 50 μM $HgCl_2$ (compare upper two curves with bottom curve). Another effect of $HgCl_2$ is an increased permeability (leak) of small solutes in vesicles containing water channels (Van Hoek et al., 1990). Figure 4A also shows that the rate of urea influx is increased (upward deflection) by lower concentrations of $HgCl_2$ than are required for the inhibition of water permeability (bottom five curves). In control studies, 100 μM $HgCl_2$ did not affect water or urea permeability in protein-free liposomes (not shown). The $HgCl_2$ concentration dependence for inhibition of water permeability and increase in urea permeability is summarized in Figure 4B. The shape of the curve for water-transport inhibition is consistent with the apparent cooperativity.

Figure 4B also shows a biphasic decrease in CHIP28 tryptophan fluorescence with increasing $HgCl_2$ concentration. Approximately 40% of the fluorescence was quenched at 5 μM $HgCl_2$, and an additional ~30% of total fluorescence was quenched with a $K_{1/2}$ of ~25 μM $HgCl_2$. The biphasic quenching plot suggests at least two sites of action of $HgCl_2$. The addition of β-mercaptoethanol (5 mM) reversed both the inhibition in P_f and the tryptophan quenching whereas EDTA (5 mM) had no effect, indicating a reversible covalent interaction (as expected from the sulfhydryl chemistry). At high [$HgCl_2$], a maximum tryptophan quenching of ~70% was observed, suggesting that two or more tryptophans in CHIP28 are quenched by $HgCl_2$. The data in Figure 4B for fluorescence quenching, P_f inhibition, and P_{urea} increase can be compared to determine whether the two apparent affinities for $HgCl_2$ quenching can be associated with functional effects. Qualitatively, the high affinity quenching and increase in P_{urea} occur at low [$HgCl_2$], whereas the low-affinity quenching and P_f inhibition occur at higher [$HgCl_2$]. However, the quenching and functional effects have different $K_{1/2}$ values, so that it is not possible to assign the two apparent mercurial affinities to separate effects on water or urea transport. There may be nonlinear coupling (e.g., apparent cooperativity) between $HgCl_2$ dose and transport function for a number of reasons, including the oligomeric assembly of CHIP28 monomers, $HgCl_2$-induced changes in CHIP28 conformation, and multisite $HgCl_2$ interactions.

To investigate whether $HgCl_2$ causes a gross change in CHIP28 conformation that is manifested by the movement of one or more tryptophans from a nonpolar to a polar environment, acrylamide was added after maximum quenching by $HgCl_2$. (Similar studies with iodide could not be performed because iodide chemically reacts with $HgCl_2$.) After quenching of 57% tryptophan fluorescence by 20 μM $HgCl_2$, the addition of 500 mM acrylamide did not quench fluorescence further. On the basis of a mathematical analysis of quenching at common vs separate sites,[2] it was concluded that $HgCl_2$ does not result in the exposure of nonpolar tryptophans to an

[2] For a quencher Q_1 acting at one site but with some fraction of fluorescence, F_u/F_o, inaccessible, $F_o/F = [1 + K_1Q_1]/[1 + (F_u/F_o) \times K_1Q_1]$, where K_1 is the Stern–Volmer constant. For two separate quenchers, Q_1 and Q_2, acting at the same site, $F_o/F = [1 + K_1Q_1 + K_2Q_2]/[1 + (F_u/F_o)(K_1Q_1 + K_2Q_2)]$. This equation predicts that the initial slope of the Stern–Volmer plot (F_o/F vs Q_2), $d(F_o/F)/dQ_2$, in the presence of Q_1 relative to that in the absence of Q_1 is $[1 + (F_u/F_o)K_1Q_1]^{-2}$, which is always ≤1. For the case of two quenchers, each of which quenches at separate sites (with fluorescence of F_{Q_1} and F_{Q_2}, respectively), $F_o/F = [(1 + K_1Q_1)(1 + K_2Q_2)]/[1 + (F_u + F_{Q_2})K_1Q_1/F_o + \{F_{Q_1} + F_u(1 + K_1Q_1)\}K_2Q_2/F_o]$. Here, the ratio of the initial slope in the presence of Q_1 to that in the absence of Q_1, $(1 + K_1Q_1)/[1 + (F_u + F_{Q_2})K_1Q_1/F_o]$, is always >1. Therefore, if the addition of a second quencher has no effect on fluorescence [$d(F_o/F)/dQ_2 < 1$], the quenchers must act at the same site.

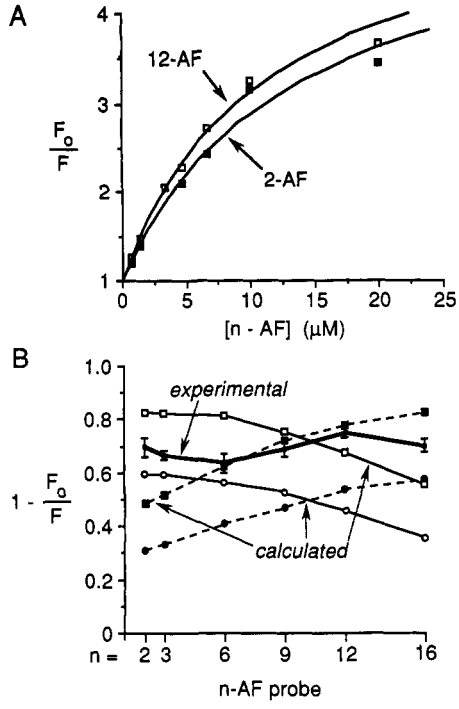

FIGURE 5: Quenching of CHIP28 tryptophan fluorescence by *n*-anthroyloxy fatty acids. Fluorescence measurements were performed as described in Materials and Methods. (A) Stern–Volmer plot for the quenching of CHIP28 (5 μg/mL) in stripped vesicles by 2-AF and 12-AF. (B) Energy-transfer efficiencies ($1 - F/F_o$) for a series of *n*-AF compounds (data labeled experimental, heavy line (■), mean ± SEM, $n = 5$ separate sets of measurements) measured at 20 μM *n*-AF. The curves labeled "calculated" were obtained from a theoretical treatment of energy transfer between a protein tryptophan and the anthroyloxy chromophore (Kleinfeld & Lukacovic, 1985). Curves are shown assuming that all of the tryptophans are located at the bilayer surface (○, □) or center (●, ■). Parameters: Forster distance, 2.2 nm; bilayer thickness, 4 nm; *n*-AF density, 26 pmol/cm²; effective protein radius, 1.1 nm (□, ■) and 1.9 nm (○, ●) (see the text for details).

aqueous environment in which acrylamide has access and that the tryptophan(s) quenched by acrylamide is also quenched by $HgCl_2$.

To determine whether the tryptophans in CHIP28 are associated with the membrane, fluorescence quenching by *n*-anthroyloxy fatty acids (*n*-AF) was measured. The *n*-AF compounds contain an anthroyloxy chromophore at specific positions along the fatty acid chain and are readily incorporated into the lipid phase of the bilayer when added from concentrated ethanolic stock solutions (Chatelier et al., 1984). The quenching of tryptophan fluorescence by the anthroyloxy chromophore by a nonradiative energy-transfer mechanism has been exploited to "map" tryptophan locations by comparison of the energy-transfer efficiencies measured for a series of *n*-AF compounds (n = 2–16 available) (Kleinfeld & Lukacovic, 1985). Figure 5A shows representative data for the dose-dependent quenching of tryptophans in CHIP28 by two of the *n*-AF compounds, where the maximum amount of *n*-AF incorporated into the lipid portion of the bilayer was under 1 mol %. The data indicate a maximum of ~80% tryptophan quenching by *n*-AF, suggesting that three or all of the tryptophans are quenched.

The experimental data (heavy line) in Figure 5B indicate a weak dependence of energy-transfer efficiency on anthroyloxy position, with the greatest efficiencies occurring at the 2 (near the surface) and 12 (deep in the bilayer) positions. These results are compared with theoretical efficiencies calculated using the model of Kleinfeld and Lukacovic (1985). The

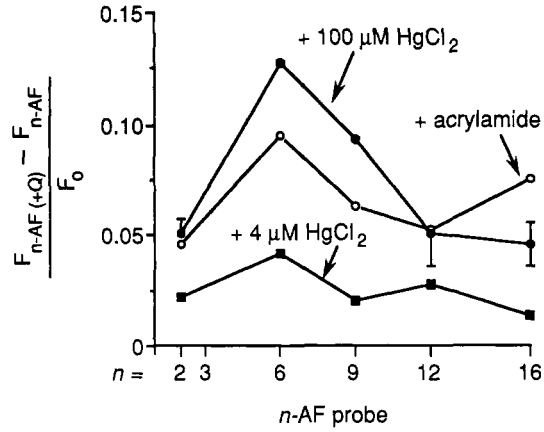

FIGURE 6: Sites of $HgCl_2$ and acrylamide quenching of CHIP28 tryptophans analyzed by *n*-AF quenching. The *n*-AF probes (13.2 μM) were incubated with CHIP28 (5 μg/mL) in stripped vesicles. Tryptophan fluorescence was measured before ($F_{n\text{-}AF}$) and after ($F_{n\text{-}AF(+Q)}$) addition of $HgCl_2$ (4 or 100 μM) or acrylamide (0.5 M). F_o is tryptophan fluorescence in the absence of quenchers.

energy-transfer efficiency was calculated for a tryptophan donor located along the axis of a transmembrane cylindrical protein and an anthroyloxy acceptor distributed throughout the plane of the lipid bilayer at a single depth specified by the *n* position. Curves were calculated for the hypothetical situation that all of the tryptophans were concentrated at the surface or center of the bilayer and for two effective protein radii (see figure legend for model parameters). The effective radius provides a measure of the closest distance between the buried tryptophan and the lipid-phase anthroyloxy chromophore. Comparison of the experimental and calculated curves suggests the following: (a) the tryptophans in CHIP28 are located preferentially at surface and deep sites within the confines of the bilayer, and (b) the tryptophans are located near the (lipid-facing) protein surface.

To obtain information about the site(s) of action of the quenchers $HgCl_2$ and acrylamide, we made use of the intrinsic depth information available from tryptophan quenching by *n*-AF. Tryptophan quenching by each of the *n*-AF probes was measured without and with the addition of $HgCl_2$ (4 and 100 μM) or acrylamide (0.5 M). The rationale for this approach is as follows: If $HgCl_2$ acts at a tryptophan(s) residing at depth n (where *n*-AF is located), then the incremental effect of $HgCl_2$ would be *smallest* in the presence of *n*-AF (because the tryptophan at position n is already quenched) and would increase progressively as the distance between the anthroyloxy chromophore and the site of $HgCl_2$ binding increases. Figure 6 shows that the addition of $HgCl_2$ or acrylamide (after *n*-AF) caused additive quenching which was maximal at the $n = 6$ position (6-AF). The simplest interpretation of these observations is that 100 μM $HgCl_2$ and acrylamide act at two sites—one near the membrane surface ($n = 2$) and the other near the center ($n = 12$) of the bilayer (see Discussion). An alternative, but less likely, explanation is that $HgCl_2$ and acrylamide each induce a conformational change in CHIP28 that results in the exposure of one or more tryptophans to *n*-AF near the $n = 6$ position (see Discussion). The difference in curve shapes corresponding to 100 (giving maximal tryptophan quenching; see Figure 4B) and 4 μM $HgCl_2$ (quenching only a high-affinity site; $n = 2$) is consistent with the possibility that an additional site deep in the membrane ($n = 12$) becomes occupied at high [$HgCl_2$].

To determine whether the highly conserved tryptophan 210 is critical for the water-transporting function of CHIP28,

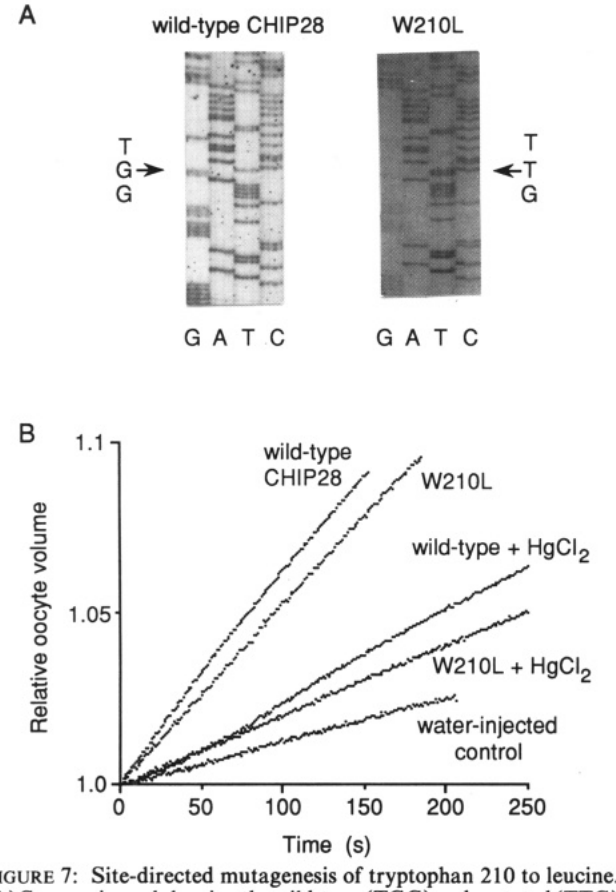

FIGURE 7: Site-directed mutagenesis of tryptophan 210 to leucine. (A) Sequencing gel showing the wild-type (TGG) and mutated (TTG) site. (B) Time course of swelling in *Xenopus* oocytes expressing wild-type and mutant (tryptophan 210 to leucine, W210L) human CHIP28. The results of a series of measurements are summarized in the text.

tryptophan 210 was mutated to leucine, and *in vitro* transcribed cRNA was expressed in *Xenopus* oocytes. Figure 7A shows the single mutated base in the sequencing gel. Figure 7B gives representative data for the time course of swelling in response to a 20-fold dilution of extracellular buffer in oocytes injected with water and cRNA encoding wild-type and mutant CHIP28. In a series of measurements, the averaged oocyte osmotic water permeability (P_f, in cm/s $\times 10^{-4}$) was 10 ± 3 ($n = 12$, water-injected); 36 ± 7 ($n = 24$, wild-type); and 32 ± 6 ($n = 30$, mutant W210L). Therefore, tryptophan 210 is not critical for the CHIP28 water-transporting function. In addition, the inhibition of oocyte P_f by 0.3 mM $HgCl_2$ was not different in oocytes expressing wild-type (13 ± 6, $n = 5$) and mutant (13 ± 3, $n = 16$) CHIP28.

DISCUSSION

The characteristics of the intrinsic tryptophan fluorescence in CHIP28 provided a set of constraints on CHIP28 structure. As shown in Figure 1, three of the four tryptophans in CHIP28 are predicted by hydropathy analysis to lie near membrane-spanning domains. The fourth (W245) is expected to lie outside of the bilayer. The analysis of tryptophan fluorescence in proteins of similar complexity (e.g., bovine heart cytochrome C oxidase, human erythrocyte hexose transporter) by selective polar and membrane-associated quenchers has provided valuable information about tryptophan environment (Eftink & Ghiron, 1981), location with respect to the bilayer surface (Hill et al., 1986), and effects of agonists on protein conformation (Pawagi & Deber, 1990). Our studies utilized the well-characterized polar quenchers iodide and acrylamide and the membrane-associated *n*-anthroyloxy fatty acids. In addition, the water transport inhibitor $HgCl_2$ was found to be a potent quencher of tryptophan fluorescence. In the discussion to follow, the tryptophan quenching data are interpreted in terms of tryptophan environment and location.

(1) All Four Tryptophans of CHIP28 Are Located in Nonpolar Environments. The emission maximum of CHIP28 tryptophan fluorescence was strongly blue-shifted at 324 nm and was not affected by the quenching compounds. In contrast, the emission maximum of MIP26 tryptophan fluorescence was at 335 nm and blue-shifted to 327 nm after quenching by iodide. It is well established that the position of the tryptophan emission maximum in proteins provides a good measure of local polarity. Maxima have ranged from 308 (azurin) to 352 nm (aqueous tryptophan), with most proteins (e.g., horse serum albumin, 342 nm; RNase T1, 324 nm; monellin, 342 nm) in the range 325–345 nm (Eftink & Ghiron, 1981). The hydrophobic environment of the tryptophans in CHIP28 is supported by the relative insensitivity to quenching by the polar compounds iodide and acrylamide, which are known to quench the fluorescence of the tryptophans to which they are accessible via aqueous-phase diffusion (Eftink & Ghiron, 1981). Although local factors such as charge effects can cause insensitivity to quenching, the fact that both charged and neutral quenchers have little effect supports the assignment of the tryptophans to a nonpolar environment. Hg^{2+}, a charged species, is able to quench the tryptophans in a nonpolar environment because it acts by binding to specific sites in CHIP28. Since the binding sites are within the membrane (see below), Hg^{2+} can quench tryptophans within the bilayer. Because Hg^{2+} quenches tryptophan fluorescence by direct binding (as opposed to a collisional mechanism for acrylamide and I^-), Hg^{2+} is able to quench tryptophan fluorescence effectively at low concentrations. Only those tryptophans which have a non-zero quantum yield are probed in these experiments. However, tryptophans with zero or very low quantum yields are unlikely to be present in proteins (Burstein et al., 1973). Therefore, it is likely that all four tryptophans contribute to the intrinsic fluorescence of CHIP28. The blue-shifted emission peak and the lack of sensitivity to polar quenchers suggest that all four tryptophans in CHIP28 reside in a nonpolar environment, either buried in a hydrophobic protein pocket or located adjacent to membrane lipid. This result was not anticipated from the predictions of hydropathy analysis.

(2) Tryptophans of CHIP28 Reside in the Membrane. The spectral data and insensitivity of tryptophan fluorescence to quenching by polar compounds do not distinguish whether the tryptophans reside in the membrane or in a hydrophobic pocket in an extramembrane-connecting domain. The strong quenching by the membrane-associated *n*-AF compounds (of up to 80%) provides evidence that three or all of the tryptophans are located in the membrane proper as bounded by the phospholipid headgroups. If the tryptophans were located outside of the bilayer, the efficiencies would be expected to be lower and show a stronger distance dependence. The shape of the energy-transfer efficiency vs n curve (Figure 5B) suggested that the tryptophans are not concentrated at any one depth in the bilayer (such as near the bilayer surface or at the center of the bilayer), but may be in multiple sites near the surface and deep in the bilayer. These conclusions were again not expected from the hydropathy analysis. While hydropathy analysis predicts that residues W11, W210, and W213 are on the edges of transmembrane α-helices, the results from this study place each of these tryptophans within the bilayer. Furthermore, the fluorescence results suggest that

W245, which is predicted by hydropathy to lie in an extramembrane region, also lies within the bilayer. Although hydropathy analysis is useful for developing a model of the topology of integral membrane proteins, the predictions of hydropathy analysis are unreliable for defining the precise boundaries of transmembrane helices. The boundaries of the putative α-helices predicted by hydropathy analysis can be refined by incorporating the results presented here.

(3) $HgCl_2$ Quenches the Fluorescence of CHIP28 but Does Not Cause a Gross Conformational Change. $HgCl_2$ is an inhibitor of the CHIP28 water channel function and was found to be a strong quencher of CHIP28 tryptophan fluorescence. Site-directed mutagenesis data (Zhang et al., 1993b) indicate that $HgCl_2$ inhibits water transport by binding covalently to cysteine 189, which is predicted to lie in an extramembrane domain between the last (near the C-terminus) and next-to-last membrane-spanning domains (see Figure 1). The biphasic quenching of CHIP28 tryptophan fluorescence and studies of the $HgCl_2$ effect on *n*-AF quenching suggest that $HgCl_2$ has two sites of action. This conclusion is supported by the observation of very different $K_{1/2}$ values for $HgCl_2$ inhibition of water permeability and increase in urea permeability. Because the functional effects of $HgCl_2$ do not closely parallel the tryptophan quenching data, it is not possible to identify the tryptophans that are quenched by low and high concentrations of $HgCl_2$. However, the ability of a low concentration of $HgCl_2$ to quench tryptophan fluorescence without inhibiting water permeability indicates that $HgCl_2$ interacts at a site other than C189 without altering the water channel function. The lack of effect of $HgCl_2$ on the tryptophan emission spectrum and on quenching by acrylamide suggests that $HgCl_2$ does not induce a gross change in CHIP28 conformation. These results are consistent with the lack of effect of $HgCl_2$ on CHIP28 secondary structure determined by circular dichroism in the preceding paper (Van Hoek et al., 1993).

(4) Tryptophans of CHIP28 May Be Located near Both the Bilayer Center Line and the Lipid Headgroups. Experiments were performed with pairs of quenchers to evaluate overlapping site specificities. There were several clear-cut observations. After maximum quenching of CHIP28 tryptophan fluorescence by any of the *n*-AF compounds, there was additional quenching by $HgCl_2$ and acrylamide. Because *n*-AF and $HgCl_2$ alone quench >50% of tryptophan fluorescence, the tryptophan(s) quenched by $HgCl_2$ was also quenched by *n*-AF. The additional quenching of tryptophan by $HgCl_2$ was maximal for 6-AF and declined monotonically for the *n*-AF probes with higher *n*. After maximum quenching of CHIP28 tryptophan fluorescence by $HgCl_2$, there was little effect of acrylamide, indicating that the tryptophan(s) quenched by acrylamide was also quenched by $HgCl_2$. These results are consistent with two models. $HgCl_2$ may interact at two sites (see the Results and Figure 6): one near the center of the bilayer and the other near the lipid headgroups. A second possibility is that binding of $HgCl_2$ to a high-affinity site causes a conformational change which repositions and exposes tryptophans at a location near the 6-AF probe. As discussed above, there is evidence for a lack of conformational change upon $HgCl_2$ binding. Further evidence in support of the first model is that both acrylamide (which also does not change CHIP28 conformation and function, see above) and $HgCl_2$ had similar effects in *n*-AF quenching studies in Figure 6.

(5) The Nonconserved Tryptophan W2 in MIP26 Is in a Polar Environment. MIP26 contains five tryptophans. Sequence alignment with CHIP28 indicates that W11, W210, and W213 of CHIP28 correspond to W10, W202, and W205 of MIP26; W2 and W34 in MIP26 have no corresponding tryptophans in CHIP28. It was found that the tryptophan emission maximum of MIP26 was red-shifted (335 nm) from that of CHIP28 (324 nm), that iodide quenched the fluorescence of MIP26 much stronger than the fluorescence of CHIP28, and that iodide quenching of MIP26 was associated with a blue shift in the MIP26 tryptophan fluorescence spectrum. These results suggest that either W2 or W34 in MIP26 is in a polar environment; analysis of MIP26 hydropathy [see Van Hoek et al. (1993)] suggests that W2 is the polar tryptophan, consistent with its position near the N-terminus.

(6) The Highly Conserved Tryptophan W210 Is Not Critical for Water-Transport Function. Previous site-directed mutagenesis studies have indicated that the highly conserved cysteine 189 is the site of $HgCl_2$ water-transport inhibition and is important for the pore properties of CHIP28 (Preston et al., 1993; Zhang et al., 1993b). To test the hypothesis that highly conserved tryptophan 210 is important for water-transport function, we mutated tryptophan 210 to leucine and assayed water transport in the *Xenopus* oocyte expression system. The tryptophan mutation had no significant effect on oocyte water permeability or on the inhibition of water permeability by $HgCl_2$. The finding that W210 is not critical for the pore function of CHIP28 is consistent with its location in a nonpolar environment.

Taken together, several lines of independent evidence suggest that all four tryptophans of CHIP28 are located within the bilayer. The *n*-AF quenching studies indicate that the tryptophans are not concentrated at a single position in the bilayer. These results were not anticipated from hydropathy analysis and must be incorporated into revised models of CHIP28 structure and membrane topology. Further measurements of the fluorescence of selected CHIP28 mutants containing single tryptophan residues would provide direct information on the location of individual tryptophans.

REFERENCES

Burstein, E. A., Vedenkina, N. S., & Ivkova, M. N. (1973) *Photochem. Photobiol. 18*, 263–279.

Chatelier, R. C., Rogers, P. J., Ghiggino, K. P., & Sawyer, W. H. (1984) *Biochim. Biophys. Acta 776*, 75–82.

Chen, R. F. (1971) *Arch. Biochem. Biophys. 142*, 552–564.

Eftink, M. R., & Ghiron, C. A. (1976) *Biochemistry 15*, 672–680.

Eftink, M. R., & Ghiron, C. A. (1981) *Anal. Biochem. 114*, 199–227.

Harris, H. W., Strange, K., & Zeidel, M. (1991) *J. Clin. Invest. 91*, 1–8.

Hasegawa, H., Zhang, R., Dohrman, A., & Verkman, A. S. (1993) *Am. J. Physiol. 33*, C237–C245.

Hill, B. C., Horowitz, P. M., & Robinson, N. C. (1986) *Biochemistry 25*, 2287–2292.

Kleinfeld, A. M., & Lukacovic, M. F. (1985) *Biochemistry 24*, 1883–1890.

Lakowicz, J. (1983) *Principles of Fluorescence Spectroscopy*, pp 347–350, Plenum Press, New York.

Pawagi, A. B., & Deber, C. M. (1990) *Biochemistry 29*, 950–955.

Preston, G. M., & Agre, P. (1991) *Proc. Natl. Acad. Sci. U.S.A. 88*, 11110–11114.

Preston, B. M., Carroll, T. P., Guggino, W. B., & Agre, P. (1992) *Science 256*, 385–387.

Preston, B. M., Jung, J. S., Guggino, W. B., & Agre, P. (1993) *J. Biol. Chem. 268*, 17–20.

Sabolic, I., Valenti, G.,Verbavatz, J. M., Van Hoek, A. N., Verkman, A. S., Ausiello, D. A., & Brown, D. (1992) *Am. J. Physiol. 263*, C1225–C1233.

Smith, B. L., & Agre, P. (1991) *J. Biol. Chem. 266*, 6407–6415.

Van Hoek, A. N., & Verkman, A. S. (1992) *J. Biol. Chem. 267*, 18267–18269.

Van Hoek, A. N., De Jong, M. D., & Van Os, C. H. (1990) *Biochim. Biophys. Acta 1030*, 203–210.

Van Hoek, A. N., Hom, M. L., Luthjens, L. H., De Jong, M. D., Dempster, J. A., & Van Os, C. H. (1991) *J. Biol. Chem. 226*, 16633–16635.

Van Hoek, A. N., Wiener, M., Bicknese, S., Miercke, L., Biwersi, J., & Verkman, A. S. (1993) *Biochemistry* (preceding article in this issue).

Verbavatz, J. M., Brown, D., Sabolic, I., Valenti, G., Van Hoek, A. N., Ma, T., & Verkman, A. S. (1993) *J. Cell Biol.* (in press).

Verkman, A. S. (1992) *Annu. Rev. Physiol. 54*, 97–108.

Wistow, G. J., Pisano, M. M., & Chepelinsky, A. B. (1991) *Trends Biochem. Sci. 16*, 170–171.

Zeidel, M. L., Ambudkar, S. V., Smith, B. L., & Agre, P. (1992) *Biochemistry 31*, 7436–7440.

Zhang, R., Skach, W., Hasegawa, H., Van Hoek, A. N., & Verkman, A. S. (1993a) *J. Cell Biol. 120*, 359–369.

Zhang, R., Van Hoek, A. N., Biwersi, J., & Verkman, A. S. (1993b) *Biochemistry 32*, 2938–2941.